ELSEVIER

Materials Science and Engineering B 123 (2005) 63–68

MATERIALS SCIENCE & ENGINEERING B

www.elsevier.com/locate/mseb

Vitrification of $K_3M_2P_3O_{12}$ (M = B, Al, Bi) NASICON-type materials and electrical relaxation studies

C.R. Mariappan [a,1], G. Govindaraj [a,*], S. Vinoth Rathan [a], G. Vijaya Prakash [b,2]

[a] Department of Physics, School of Physical, Chemical and Applied Sciences, Pondicherry University, R.V. Nagar, Kalapet, Pondicherry 605014, India
[b] School of Physics and Astronomy, University of Southampton Highfield, Southampton S017 1BJ, UK

Received 28 March 2004; received in revised form 23 November 2004; accepted 22 June 2005

Abstract

Vitreous phases of $K_3M_2P_3O_{12}$ (M = B, Al, Bi) NASICON-type materials are prepared and their electrical properties are investigated over a frequency range from 42 Hz to 1 MHz and at different temperatures. An anomalous diffusion model (ADM) is applied to discuss the ac conductivity, permittivity and electric modulus of the NASICON-type glasses. The ADM is used to extract the dc conductivity and relevant physical parameters, namely, crossover length and relaxation frequency in the ion diffusion process. The dc conductivities and relaxation frequencies are thermally activated, with activation energies found to be in the range 0.70–0.82 eV. The frequency- and temperature-dependent conductivity spectra of individual glasses can be superimposed by means of the Summerfield scaling.
© 2005 Elsevier B.V. All rights reserved.

Keywords: NASICON-type glasses; ac conductivity; Anomalous diffusion model; Electric modulus spectroscopy; Scaling analysis

1. Introduction

During the last few years, much effort has been devoted to find new solids with high ionic conductivity for applications in solid state batteries, fuel cells, sensors, etc. [1]. The general formula of a phosphate network system is $A_xM_yP_3O_{12}$, where A is an alkali ion and M is one or more ions in tri, tetra, or pentavalent state. The monovalent A ions can easily migrate in the lattice with low activation energy [2,3]. This family of crystalline phosphates (often referred to as NASICON, acronym for 'Na' superionic conductors) is uniquely identified as tailor-made materials, capable of accommodating a wide range of compositional variation, thereby offering flexibility of physical and electrical properties [3–6].

In recent years, titanium based NASICONs have received great deal of scientific attention. These crystallites (of the formula of $A_{1+x}M_xTi_{2-x}P_3O_{12}$ (AMTP), where A = Na or Li, and M is trivalent cations) show enhanced electrical conductivity features upon partial substitution of Ti^{4+} by trivalent cations (M^{3+}, such as Al, Ga, In, Sc, Y, La, Cr or Fe) [7–10]. The maximum conductivity yet obtained is about $\sim 10^{-3}$ S cm^{-1} for $Li_{1.3}M_{0.3}Ti_{1.7}P_3O_{12}$, where M is a trivalent cation Al or Sc. Only the low trivalent cation titanium based materials have been investigated. However, applicability of these NASICON polycrystalline as solid electrolytes is limited due to Ti^{4+}/Ti^{3+} reduction and the large grain boundary contribution. Recent reports suggest that such disadvantages could be conveniently minimized by vitrification and avoiding Ti of such NASICON composites [11,12].

It is also interesting to consider the vitrification capability of NASICON composites and to examine the electrical properties. Extensive studies of both vitreous and crystalline binary phosphates with NASICON chemistry, containing mostly transition metal ions (valencies 4 or 5) or non-transition metals like Ge, show significant differences in electrical properties between glassy and crystalline forms [13]. The vitreous forms of fully trivalent (M site) cation-containing binary phosphate NASICONs provide good systems for a systematic examination of elec-

* Corresponding author. Tel.: +91 413 2655991x405; fax: +91 413 2655265.
E-mail address: ggraj_7@yahoo.com (G. Govindaraj).
[1] Present address: Laboratoire des Oxydes et Fluorures (UMR 6010 CNRS), Universite du Maine, 72085 Le Mans Cedex 9, France.
[2] Present address: Department of Physics, Indian Institute of Technology, New Delhi 110016, India.

0921-5107/$ – see front matter © 2005 Elsevier B.V. All rights reserved.
doi:10.1016/j.mseb.2005.06.022

trical relaxation processes, and such systems are scarcely reported.

In this work, we report the synthesis, characterization and electrical relaxation processes in vitreous forms of $K_3M_2P_3O_{12}$ (M = B, Al, Bi) NASICONs. To the best of our knowledge, these materials have not previously been investigated. Electrical relaxation processes of the NASICON-type glasses are investigated and analyzed using an anomalous diffusion model. We also present the time-temperature superposition principle, the so-called Summerfield scaling approach, of conductivity spectra of NASICON-type glasses.

2. Experimental

The vitreous materials $K_3B_2P_3O_{12}$ (KBP), $K_3Al_2P_3O_{12}$ (KAP), and $K_3Bi_2P_3O_{12}$ (KBiP) were prepared by a solid-state reaction from K_2CO_3, B_2O_3, Al_2O_3, Bi_2O_3 and $NH_4H_2PO_4$. The KAP system was prepared by taking stoichiometric quantities of K_2CO_3, Al_2O_3, and $NH_4H_2PO_4$ and the overall reaction for KAP formation is given by:

$$3/2K_2CO_3 + Al_2O_3 + 3NH_4H_2PO_4 \xrightarrow{\Delta} K_3Al_2P_3O_{12} + 3NH_3 + 9/2H_2O + 3/2CO_2$$

The synthesis of the samples was as follows: (i) the calculated amounts of the starting materials were ground in an agate mortar for 45 min; (ii) the mixture was placed in a silica crucible and slowly heated in an electric furnace up to 523 K, further heated and held at a temperature of 623 K for 6 h in order to ensure the total decomposition of the reagents; (iii) after cooling the sample to room temperature, the mixture was again ground for 45 min in an agate mortar and heated in a silica crucible for ∼16 h at the temperature range of 923–1023 K without melting the mixtures; (iv) the sample was heated further in the range of 1173–1273 K to melt the sample and stirred for 5–10 min to ensure homogeneity; (v) finally, the melt was poured into a stainless steel plate and quenched by pressing with another stainless steel plate at room temperature.

These systems were characterized by X-ray diffraction (XRD), differential scanning calorimetry (DSC), Fourier transform infrared (FTIR) and ac electrical conductivity measurements. XRD spectra were recorded for all the samples by using a Rigaku miniflex X-ray diffractometer with monochromatic Cu Kα radiation at glancing angles between 5° and 65°. The DSC measurements were carried out using a Mettler Toledo DSC 821^e instrument and the temperature was varied from 308 to 798 K at a rate of 10 K/min. FTIR spectra were recorded in the wave number range 1600–400 cm^{-1} using the KBr pellet method in a Shimadzu FTIR-8700 spectrophotometer at room temperature. Measurements had a spectral resolution of 4 cm^{-1} and were averaged over 40 scans.

The samples for electrical conductivity measurements were made by cutting the prepared glasses into pellets of ∼10 mm diameter and ∼1.5–2.0 mm thickness. Both sides of the samples were ground and polished. Silver paint was pasted on to the parallel surfaces of the polished sample and the sample was fixed in the spring loaded sample holder. Parallel conductance and capacitance for all the compounds were measured using a Hioki 3532-50 LCR Hitester in the frequency range of 42 Hz to 1 MHz and in the temperature range from 300 to 470 K. The measurements were carried out in an under vacuum. Prior to the electrical conductivity measurements, the samples were heated at 373 K in a spring loaded sample holder to allow stabilization of the electrodes and then the samples were cooled. The Lab-Equip package program was used to control electronically the temperature and measurement processes.

3. Results and discussion

X ray diffraction (XRD) patterns were recorded for all the samples understudy and they (not shown here) do not display any features, suggesting the amorphous nature of the samples. Fig. 1(a) shows the FTIR absorption spectra for the different NASICON-type vitreous materials. Possible infrared band assignments are indicated by arrow mark in the figure. Table 1 shows corresponding absorption assignment values. These bands are assigned to the various vibrational contributions of the basic phosphates [14–19]. The entire region between 1200 and 400 cm^{-1} dominantly by the vibrations of the PO_4 tetrahedra. The spectra are similar for different alkali members for common M ion [20] but for different M ions spectra show less similarity for the same alkali ion, implying that M ions play a more significant role than alkali ion in the

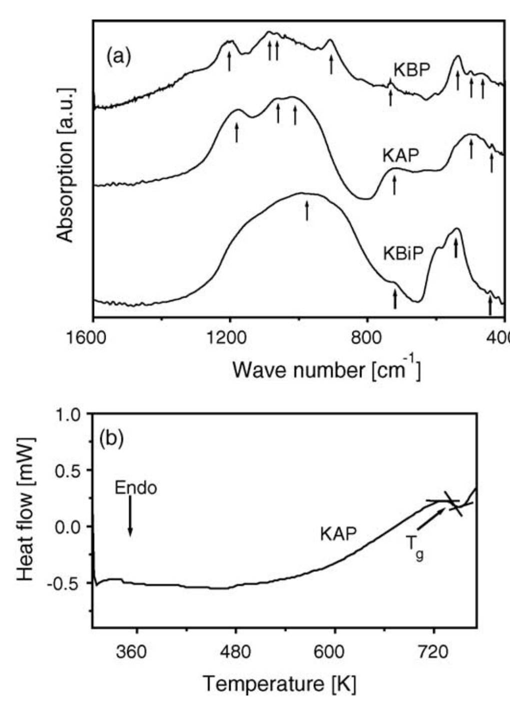

Fig. 1. (a) FT-IR spectra of NASICON-type glasses. (b) DSC thermogram for KAP glass.

Table 1
FTIR absorption bands (in cm^{-1}) and attributions for the NASICON-type vitreous materials

Sample	Harmonics of P–O–P bending	P–O–P stretching	$PO_3{}^{2-}$ ionic	$PO_4{}^{3-}$ ionic	$P_2O_7{}^{4-}$ pyrophosphate
$K_3B_2P_3O_{12}$	466, 497, 534	729	906	1027, 1085	1189
$K_3Al_2P_3O_{12}$	499	717	–	1018, 1064	1175
$K_3Bi_2P_3O_{12}$	441, 538	723	–	997	–

Table 2
Glass transition temperature (T_g), dc conductivity activation energy (E_σ), conductivity elaxation frequency activation energy (E_ω), frequency exponent (n), cross over length (ξ) and KWW stretched exponent (β), for the NASICON-type samples

Name of the sample	T_g (K)	E_σ (eV) $\pm$ 0.02	E_ω (eV) $\pm$ 0.02	$n \pm 0.03$	ξ (Å)	$\beta \pm 0.02$
$K_3B_2P_3O_{12}$	678	0.71	0.70	0.66	0.69	0.57
$K_3Al_2P_3O_{12}$	747	0.75	0.74	0.63	0.80	0.63
$K_3Bi_2P_3O_{12}$	688	0.82	0.82	0.60	0.91	0.65

structure of the glass. The spectra further suggest the fully vitrified samples, as there are no traces of the initial precursors (absence of carbonate absorption peaks, typically observable in the 1500–1400 cm^{-1} region). The DSC thermogram was recorded for all the samples and it is shown in Fig. 1(b) at scan rate of 10 K/min. The endothermic and exothermic peaks observed in the DSC are corresponds to the glass transition and crystallization respectively for the present amorphous material. The glass transition (T_g) temperatures of all vitreous samples are shown in Table 2.

3.1. Electrical conductivity studies

The frequency dependent conductivity in KBP at various temperatures is shown in Fig. 2(a). The conductivity is found to be frequency independent in the low frequency regime, suggesting that the ions perform uncorrelated and random hopping motions leading to a macroscopic transport or dc conductivity [21]. In the high frequency region, where the power law dispersion, $\sigma(\omega) \propto \omega^n$, is observed, indicating correlated forward–backward hopping of ion motion [22]. The range of low frequency conductivity plateau is found to increase with temperature, while the temperature dependency is less prominent in the high frequency region. The real part of the dielectric permittivity $\varepsilon'(\omega)$, as shown in Fig. 2(b) for KBP at different temperatures, follows a well-known non-Debye behavior, $\omega^{(n-1)}$, in the high frequency region [21]. The $\varepsilon'(\omega)$ increases with decreasing frequency, approaching a limiting value, ε_s, which is associated with polarization resulting from the alignment of the dipoles along the direction of the electric field at low frequencies. At high temperatures, the limiting value, ε_s, increases sharply, possibly due to the contribution from the charge accumulation at the electrode-sample interface [21].

Recently, a number of theoretical models have been proposed based on anomalous diffusion in the analysis of ac conductivity [22–26]. We have taken the anomalous diffusion model (ADM) proposed by Sidebottom et al. for ac conductivity and permittivity. This model successfully eliminates the numerical fitting uncertainty in the high frequency region of electric modulus. It also provides other important parameters, namely, length and time scales involved in the diffusion process. The frequency dependent conductivity $\sigma(\omega)$ and the real part of the dielectric permittivity $\varepsilon'(\omega)$ can be expressed as [27]:

$$\sigma(\omega) = \sigma_{dc}[1 + h(n)\cos(n\pi/2)(\omega/\omega_\sigma)^n], \quad (1)$$

$$\varepsilon'(\omega) = \varepsilon_\infty[1 + h(n)\sin(n\pi/2)(\omega/\omega_\sigma)^{n-1}], \quad (2)$$

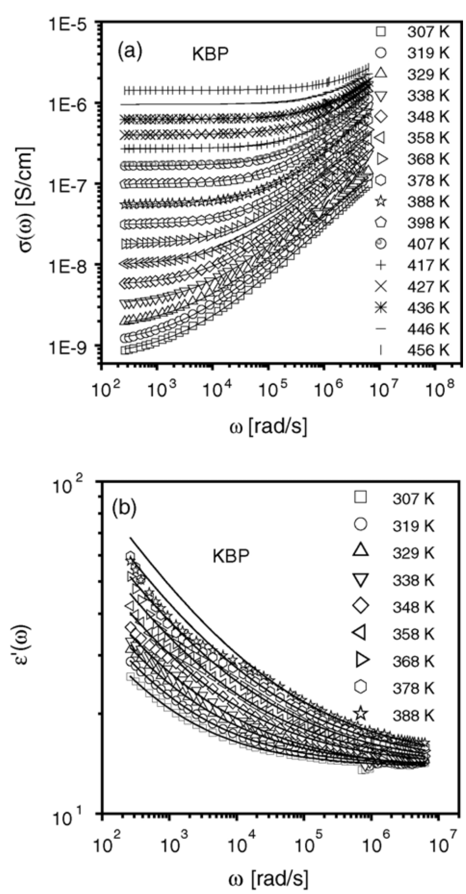

Fig. 2. (a) ac conductivity of for KBP at different temperatures. The solid lines are the fits to Eq. (1). (b) ac real part of permittivity of KBP at selected temperatures. The solid lines are the fits to Eq. (2).

with $h(n) = f^n g(n)$, $g(n) = \Gamma(2 - n)$

$$\omega_\sigma = \mathrm{f}\omega_c \text{ (or) } \omega_\sigma = \sigma_{dc}/\varepsilon_\infty\varepsilon_0, \qquad \sigma_{dc} = K\xi^2\omega_c, \quad K = e^2_{n_{c\rho}}/6kT, \tag{3}$$

where σ_{dc} is the dc conductivity, ω_σ the conductivity relaxation frequency, ε_∞ the high-frequency dielectric permittivity, ε_0 the permittivity at free space, ξ is cross over length, n the frequency exponent ($0 < n < 1$), ω_c the crossover frequency, e is electronic charge, and $n_{c\rho}$ is the number density of charge carrier. Eqs. (1) and (2) are used to fit the measured ac conductivity and the real part of permittivity data by the non-linear least square fitting method and the parameters σ_{dc}, ω_c, ε_∞ and n are extracted. Both equations fit well with the experimental data shown in Fig. 2(a) and (b) and the parameters evaluated from the above fitting are represented in Table 2. The crossover length parameter (ξ) involved in the diffusion process is increasing with the M site cation size. Furthermore, the obtained n values (0.60–0.66) are universally characteristic of the non-Debye behavior of materials. The n value, together with the small value of ξ, supports the Coulombic interaction-based diffusion models such as the jump relaxation model and the Coulomb-interacting lattice gas model [22,28].

The parameters σ_{dc} and ω_σ, extracted from the above fits are strongly dependent on temperature and show a general trend of KBP > KAP > KBiP. These features suggest strong M-site ion radius dependence and possible thermally activated drift mobility of ions, according to hopping mechanism [29]. Fig. 3(a) and (b) show the plots of $\ln(\sigma_{dc}T)$ versus $1000/T$ and $\ln(\omega_\sigma)$ versus $1000/T$, respectively, for different NASICON-type glasses. This temperature dependency is found to obey the Arrhenius equations:

$$\sigma_{dc}T = \sigma_0 \exp(-E_\sigma/kT), \tag{4}$$

$$\omega_\sigma = \omega_0 \exp(-E_\omega/kT), \tag{5}$$

where σ_0 is the dc conductivity pre-exponential factor, E_σ is the dc conductivity activation energy for mobile ions, ω_0 is the pre-exponential of the conductivity relaxation frequency, and E_ω is the activation energy for the conductivity relaxation frequency.

The activation energies, E_σ and E_ω are determined using Arrhenius equation by linear regression and are shown in Table 2. The close match between E_ω and E_σ indicates that the charge carriers have to overcome the same energy barrier in both conduction and relaxation processes. Both these activation energies show increase with the size of M site ion i.e., with a general trend of KBP < KAP < KBiP. It is also interesting to note that the strongly temperature dependant parameters σ_{dc} and ω_σ, show a general trend of KBP > KAP > KBiP, thus suggesting the strong correlation between the activation energies and the above parameters.

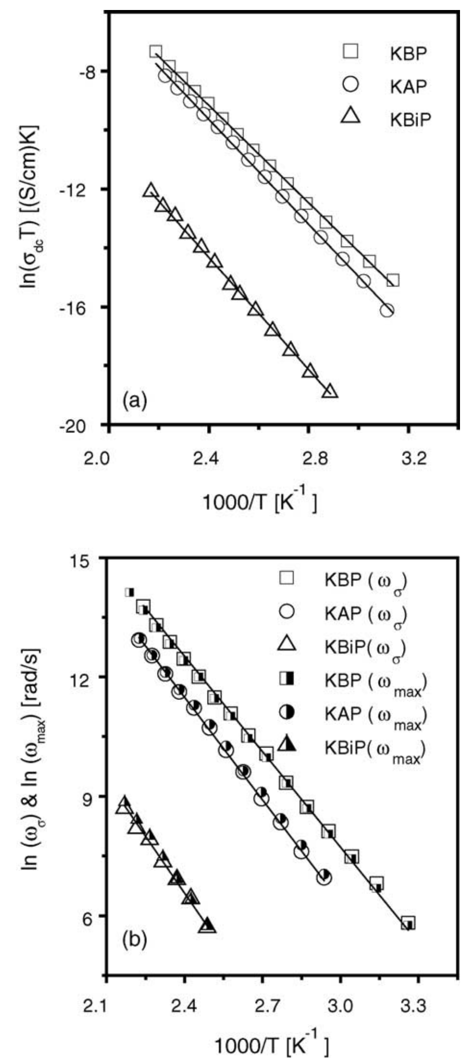

Fig. 3. (a) dc conductivity vs. reciprocal temperatures for the NASICON type glasses. The solid lines are the fits to Eq. (4). (b) Temperature dependence of conductivity relaxation frequency for NASICON type glasses. The solid lines are the fits to Eq. (5).

3.2. Electric modulus analysis

The dielectric response of the materials can alternatively be analyzed in terms of complex electric modulus $M^*(\omega)$, with the added advantage of suppressing the electrode polarization effects [30–32]. Fig. 4(a) and (b), are representative of curves of the real ($M'(\omega)$) and imaginary ($M''(\omega)$) parts of the electric modulus at different temperatures for one of the glasses, KBP. In Fig. 4(a), $M'(\omega)$ attains a constant value at high frequencies for all temperatures and tends to zero at low frequencies, indicating negligible electrode polarization [32]. The $M''(\omega)$ spectra in Fig. 4(b) show slightly asymmetric peak which shifts towards higher frequencies as temperature increases.

The dielectric relaxation process, in general, can be represented by the numerical Laplace transform of the Kohlrausch–Williams–Watts (KWW) decay function,

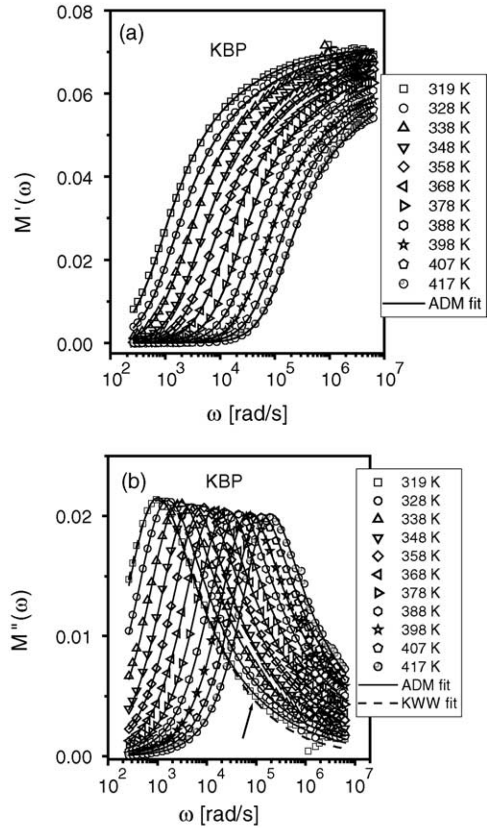

Fig. 4. Isothermal modulus spectra for KBP at several temperatures (a) $M'(\omega)$ and (b) $M''(\omega)$, the dashed line is fits to KWW equation. The solid curves are the fits to ADM.

$\phi(t) = \exp[-(t/\tau)^{\beta}]$, where the exponent β characterizes the degree of non-Debye behavior and τ is the conductivity relaxation time [30].

Recently, Bergman has modified the KWW function fitting approach, allowing direct analysis in the frequency domain [33,34]. The imaginary part of the $M''(\omega)$ has been approximated as (for $\beta \geq 0.4$):

$$M''(\omega) = \frac{M''_{\max}}{(1-\beta) + (\beta/1+\beta)[\beta(\omega_{\max}/\omega) + (\omega/\omega_{\max})^{\beta}]}, \tag{6}$$

where $M''_{\max}$ is the peak maximum of the imaginary part of the modulus and $\omega_{\max}(=1/\tau)$ is the peak frequency of the imaginary part of the modulus. We analyzed our experimental data using this modified KWW approach (Eq. (6)) and although the model represents the usual features of M'', the fit is unsuccessful in the higher frequency region (indicated by arrow mark in Fig. 4(b)). A representative of the fitting is shown as a dashed line in Fig. 4(b). Corresponding β values used in the fits are displayed in Table 2.

As an alternative approach, we used power-law expression suggested in the anomalous diffusion model (ADM), discussed previously in this paper, to avoid the uncertainty of fitting in $M''(\omega)$ in the high frequency region. Both the real and imaginary parts of electrical modulus can be represented in terms of $\sigma(\omega)$ and $\varepsilon'(\omega)$ as:

$$M'(\omega) = \varepsilon'(\omega)/(\varepsilon'^{2}(\omega) + (\sigma(\omega)/\omega)^{2}), \tag{7}$$

$$M''(\omega) = (\sigma(\omega)/\omega)/(\varepsilon'^{2}(\omega) + (\sigma(\omega)/\omega)^{2}). \tag{8}$$

The results are shown in Fig. 4(b) for KBP at selected temperatures. In this figure, we show both the fittings of models ADM (solid line) as well as KWW (dashed line). It is clear from Fig. 4(b) that the ADM model play an important role at the high frequency region and therefore a fairly reasonable fit is possible in the high frequency wing of the $M''(\omega)$. The KWW fitting $\omega_{\max}$ values and ADM fitting ω_{σ} values are almost equal and they are plotted in Fig. 3(b) as a function of temperature. In general, both the models KWW and ADM, provide the same quantitative macroscopic information regarding the conductivity relaxation, i.e., steady state ion transport processes at short length scales, rather than details of structure.

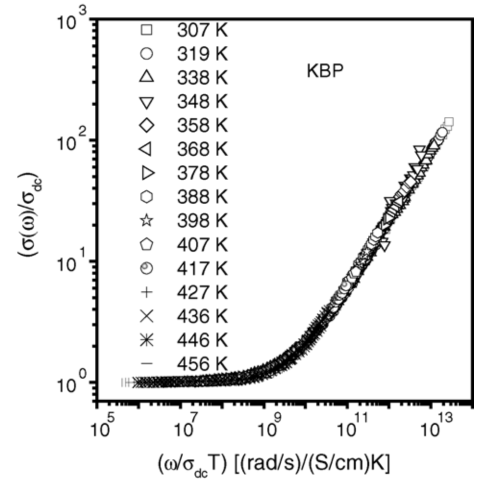

Fig. 5. Summerfield scaling for conductivity spectra of KBP.

3.3. ac conductivity scaling studies

It is a general practice to correlate the universal features of the physically measurable properties of materials, as this often facilitates the comparison of structurally diverse materials and, hence, the extrapolation of unknown quantities. For instance, based on Arrhenius temperature dependence, it is possible to scale the ac conductivity at different temperatures to a single curve by choosing an appropriate scaling quantity [25,35–37]. Here, the scaling in ac conductivity for NASICON-type glasses is studied by scaling both the ac conductivity axis by σ_{dc}, and the frequency axis by $\sigma_{dc}T$ at different temperatures [36]. This so-called Summerfield scaling uses the directly measurable quantities σ_{dc} and T as the scaling parameters. Fig. 5 shows scaled conductivity spectra for KBP glass. The scaled ac conductivity data are collapsed into a single curve, similar to the features obtained for other glassy systems. This study further emphasizes the merit of our systems and suggests that the conductivity relaxation mechanism is independent of temperature.

4. Conclusions

The new $K_3M_2P_3O_{12}$ (M = B, Al, Bi) NASICON-type materials were successfully vitrified and the glassy nature is further characterized by XRD, DSC and FTIR techniques. The electrical properties of the glasses were studied over wide range of temperature and ac frequency. The anomalous diffusion model is used to study the power law dependence of conductivity and permittivity and to evaluate various important parameters of NASICON-type glasses. In general, the cross over lengths, ξ and activation energies show M site cation size dependency in all systems under the present investigation. The electrical modulus spectra are analyzed by both KWW and ADM models, enabling further discussion of the model validity, particularly at the high frequency wing of the modulus spectra. A scaling approach between the ac conductivity and the temperature further appreciates the merit of our systems, and also shows generalized features of other reported glasses.

Acknowledgments

The financial support from CSIR, Government of India, Research Projects F. 03/0973/02 EMR-II is gratefully acknowledged for this work. One of the authors (C.R.M) thanks the CSIR, Government of India, for the award of a Senior Research Fellowship. We also thank profusely Dr. Chris Finlayson, University of Southampton, UK, Dr. Jodi-Anne Wood and Dr. C.R. Ramanathan, University of Connecticut, USA, for critical reading.

References

[1] M.D. Ingram, A.H. Jean Robertson, Solid State Ionics 94 (1997) 49; J.B. Goodenough, Solid State Ionics 94 (1997) 17.
[2] H.Y.-P. Hong, Mater. Res. Bull. 11 (1976) 173; J.B. Goodenough, H.Y.-P. Hong, J.A. Kafalas, Mater. Res. Bull. 11 (1976) 203.
[3] J. Alamo, R. Roy, J. Mater. Sci. 21 (1986) 444.
[4] S. Wong, P.J. Newman, A.S. Best, K.M. Nairn, D.R. MacFarlane, M. Forsyth, J. Mater. Chem. 8 (1998) 2199.
[5] A. El Jazouli, C. Parent, J.M. Dance, G. Le Flem, P. Hagenmuller, J.C. Viala, J. Solid State Chem. 74 (1988) 377; S. Barth, R. Olazcuaga, P. Gravereau, G. Le Flem, P. Hagenmuller, Mater. Lett. 16 (1993) 96.
[6] C.R. Mariappan, G. Govindaraj, Mater. Sci. Eng. B 94 (2002) 82; C.R. Mariappan, G. Govindaraj, Solid State Ionics 147 (2002) 49.
[7] H. Aono, E. Sugimoto, Y. Sadaoka, N. Imanaka, G.-Y. Adachi, J. Electrochem. Soc. 137 (1990) 1023; H. Aono, N. Imanaka, G.Y. Adachi, Acc. Chem. Res. 27 (1994) 265; H. Aono, N. Imanaka, G.Y. Adachi, Adv. Mater. 8 (1996) 127.
[8] K. Arbi, S. Mandal, J.M. Rojo, J. Sanz., Chem. Mater. 14 (2002) 1091.
[9] F.E. Mouahid, M. Bettach, M. Zahir, P. Maldonado-Manso, S. Bruque, E.R. Losilla, M.A.G. Aranda, J. Mater. Chem. 10 (2000) 2748.
[10] F.E. Mouahid, M. Zahir, P. Maldonado-Manso, S. Bruque, E.R. Losilla, M.A.G. Aranda, A. Rivera, C. Leon, J. Santamaria, J. Mater. Chem. 11 (2001) 3258.
[11] L. Moreno-Real, P. Maldonado-Manso, L. Leon-Reina, E.R. Losilla, F.E. Mouahid, M. Zahir, J. Sanz, J. Mater. Chem. 12 (2002) 3681.
[12] C.J. Leo, B.V.R. Chowdari, G.V. Subba Rao, J.L. Souquet, Mater. Res. Bull. 37 (2002) 1419.
[13] K.C. Sobha, K.J. Rao, Solid State Ionics 81 (1995) 145; K.C. Sobha, K.J. Rao, J. Non-Cryst. Solids 201 (1996) 52.
[14] A.A. Higazy, B. Bridge, J. Mater. Sci. 20 (1985) 2345.
[15] K. Nakamoto, Infrared and Raman Spectra of Inorganic and Coordination Compounds, Part A. Theory and Applications in Inorganic Chemistry, Wiley, New York, 1997.
[16] C. Dayanand, G. Bhikshamaiah, V. Jayatyagaraju, M. Salagram, A.S.R. Krishnamurthy, J. Mater. Sci. 31 (1996) 1945.
[17] I.N. Chakraborty, R.A. Condrate Sr., Phys. Chem. Glasses 26 (1985) 68.
[18] D.E.C. Corbridge, E.J. Lowe, J. Chem. Soc., Part I (1954) 493.
[19] K.J. Rao, K.C. Sobha, S. Kumar, Proc. Indian Acad. Sci. 113 (2001) 497.
[20] C.R. Mariappan, G. Govindaraj, S. Vinoth Rathen, G. Vijaya Prakash, Mater. Sci. Eng. B 121 (2005) 2.
[21] A.K. Jonscher, Dielectric Relaxation in Solids, Chelsea Dielectric Press, London, 1983.
[22] K. Funke, Prog. Solid State Chem. 22 (1993) 111.
[23] K. Funke, R.D. Banhatti, S. Brucker, C. Cramer, C. Krieger, A. Mandanici, C. Martiny, I. Ross, Phys. Chem. Chem. Phys. 4 (2002) 3155.
[24] J.C. Dyre, T.B. Schroder, Phys. Stat. Sol. (b) 230 (2002) 5.
[25] B. Roling, Phys. Chem. Chem. Phys. 3 (2001) 5093.
[26] P. Maass, J. Petersen, A. Bunde, W. Dieterich, H.E. Roman, Phys. Rev. Lett. 66 (1991) 52.
[27] D.L. Sidebottom, P.F. Green, R.K. Brown, Phys. Rev. Lett. 51 (1995) 2770.
[28] P. Maass, J. Petersen, A. Bunde, W. Dieterich, H.E. Roman, Phys. Rev. Lett. 66 (1991) 52.
[29] D.P. Almond, G.K. Duncan, A.R. West, Solid State Ionics 9/10 (1983) 277; D.P. Almond, G.K. Duncan, A.R. West, J. Non-Cryst. Solids 74 (1985) 285.
[30] C.T. Moynihan, L.P. Boesch, N.L. Laberge, Phys. Chem. Glasses 14 (1973) 122.
[31] J.R. Macdonald, Solid State Ionics 133 (2000) 79; J.R. Macdonald, J. Appl. Phys. 90 (2001) 153.
[32] P.B. Macedo, C.T. Moynihan, R. Bose, Phys. Chem. Glasses 13 (1972) 171.
[33] R. Bergman, J. Appl. Phys. 88 (2000) 1356.
[34] C. Karlsson, A. Mandanici, A. Matic, J. Swenson, L. Börjesson, J. Non-Cryst. Solids 307–310 (2002) 1012.
[35] J.C. Dyre, T.B. Schrøder, Rev. Mod. Phys. 72 (2000) 873.
[36] S. Summerfield, Philos. Mag. B 52 (1985) 9; N. Balkan, P.N. Butcher, W.R. Hogg, A.R. Long, S. Summerfield, Philos. Mag. B 51 (1985) 7.
[37] C.R. Mariappan, G. Govindaraj, J. Mater. Sci. Lett. 21 (2002) 1401.